A Novel Application of Time Reversed Acoustics: Salt Dome Flank Imaging Using Walk Away VSP Surveys

Mark Willis[1], Rongrong Lu[1], Daniel R. Burns[1], Nafi Toksöz[1], Xander Campman[1], and Martijn de Hoop[2]

[1] Earth Resources Laboratory, Massachusetts Institute of Technology, Cambridge, MA 02139
[2] Center for Wave Phenomena, Colorado School of Mines, Golden, CO 80401

Abstract

In the past few years, there has been considerable research and interest in a topic known by various names, such as Time Reverse Acoustics (TRA), Time Reverse Mirrors (TRM), and Time Reverse Cavities (TRC), which exploits reciprocity and the time symmetric property of the wave equation. Very little of this work has been directed at the seismic exploration imaging problem. In fact, most of the work has had application in sonar, medical and non-destructive testing applications. Here we present some initial results of applying this technology to the seismic imaging of a salt dome flank. We create a set of synthetic traces representing a multi-level, walk away VSP for a model composed of a simplified Gulf of Mexico vertical velocity gradient and an embedded overhanging salt dome. To process these data, we first apply the concepts of TRA to the synthetic traces. This creates a set of stacked traces without having to perform any velocity analysis or complicated processing. Each of these stacked traces is equivalent to the output of a spatially coincident, or zero offset, down hole source and receiver pair. Thus we have the equivalent of a zero offset seismic section as if it were collected from down hole sources and receivers. After having applied the TRA concepts, we then apply conventional post stack depth migration to this zero offset section to produce the final image of the salt dome flank. Our results show a very good image of the salt. In fact, the image created is nearly identical to an image actually using data from down hole, zero offset source and receiver pairs. The simplicity of the TRA implementation provides a virtually automated method to create a stacked section as if it had been collected from the reference frame of the borehole containing the VSP survey.

1. Introduction

Time Reverse Acoustics (TRA) is a part of a set of closely related technologies which have been evolving over the past few years by researchers in several fields. As such, it is been referred to by terms like Time Reverse Mirrors, Time Reverse Acoustics, and Time Reverse Cavities (e.g. Derode et al., 2000; Fink, 2000, 2001; Jonsson et al, 2004). Much of this work pertains to measuring a recorded wave field from a sound source in a physical experiment, time reversing the recorded pressures, and then re-injecting the time reserved waveforms into the medium at the recording locations. The result of this process effectively back propagates the signal to the original sound source location. This is highly effective, for example, in deriving the beam steering parameters to focus a blast of ultrasonic sonic energy created by an array of sources located outside of a person's body to heat and destroy internal tumors in medical treatment applications. In this paper we extend the notion of time reverse acoustics to the seismic exploration problem.

Since the 1980's there has been much work done on the topic of reverse time migration of seismic data (e.g. Whitmore, 1983; Baysal et al, 1983; Levin, S.A., 1984; Hellman et al, 1986; Chang and McMechan, 1987). However, it is important to understand that reverse time migration (RTM) is distinctly different from TRA. Both are built upon the notion of the time symmetric properties of the wave equation - we can run the wave equation forward and backward in time without any loss of accuracy. RTM uses a numerical modeling scheme, such as finite differences or Kirchhoff extrapolation, to implement running the wave equation backward in time and then invokes an imaging condition to create the migrated image. In contrast, TRA implements running the wave equation backward in time, typically to only a single point in the medium, by using the sum of auto or cross correlations of the recorded signals. TRA does not produce an image, but rather a new waveform representing the history of the motion of the medium at that back propagated location. The TRA literature is mainly concerned with collapsing all the energy back to the source point in the medium. Here we show that by applying TRA concepts to a walk away

VSP survey, we can create an equivalent down hole, zero offset seismic survey as if the sources and receivers were located in the VSP borehole.

We first create seismic data representing a multi-level, 2D walk away VSP survey. The velocity model was chosen to be representative of the Gulf of Mexico with a typical vertical velocity gradient and a large, overhanging salt dome. Next, by applying TRA concepts we are able to collapse all of the 30,000 recorded traces to 100 autocorrelated and summed traces representing the equivalent of a stack section as if it were acquired only from down hole sources and receivers. We then migrate these 100 traces with a conventional post stack reverse time migration algorithm and obtain a very good image of the salt dome flank. The comparison of this image with that obtained by migrating the actual down hole, zero offset VSP traces is extremely good.

2. Principles of Time Reverse Acoustics

While the literature uses many different approaches to explain and derive the various theories and technologies related to TRA, we will simplify all of them down to two basic principles: 1) the time symmetry of the wave equation, and 2) the estimation and use of the Greens function of the medium. To this we will add our own "principle" about the value of the back propagated signal.

2.1 Principle 1 – time symmetry of the wave equation

The first basic principle of TRA is that the acoustic and elastic wave equations are symmetric with respect to time. Suppose we were to observe the outward expanding wave field created from a point source located inside a medium. Further, suppose we capture the wave field at all points, and for all time on an enclosed contour surrounding the source, but at some distance away. If we then start a new simulation by time reversing the recorded signals and subsequently re-injecting them into the medium at the recording locations, we would observe all the energy propagate completely back to the original source location. A movie can be made from the snap shots of the original outward propagating wave field. If this movie is played backward in time, it would be identical to a movie made from the snap shots of the back propagated wave field. Thus we can run the movie of the outward expanding wave field from the source forward and backward and the wave field will obey the wave equation in each direction. This principle applies equally to both numerical modeling and physical experiments – we can propagate a signal to and from its original source position and an arbitrary contour surrounding it using the wave equation.

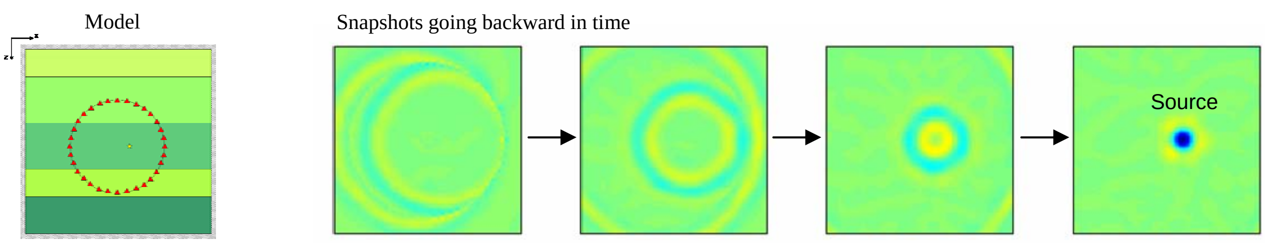

Figure 1. A simple layered earth model (left most panel) shown with a point source at the location of the yellow star, and receivers, shown as red triangles, located on a circular contour at some distance around the source. The other four panels show snap shots of the recorded wave field being back propagated in time to the source location.

To demonstrate this first principle, we create a simple example showing the symmetry of the wave equation in time. The left panel in Figure 1 shows a simple layered earth model with a seismic source indicated by the yellow star and a circular ring of about 60 receivers indicated by the red triangles. We used an elastic 2D finite difference modeling code to create the seismograms at each of these receiver locations using an explosive source function. The traces were then reversed in time and input into the same model at each corresponding receiver position. Snap-shots of the back propagating wave field are shown in the remaining panels of Figure 1. Each frame then marches the wave field backward in time, back to the source location. Clearly shown in the fourth snap shot frame is the convergence of the back propagated field to the source location. This convergence is both in time and in space, to the lateral position of the source and its proper depth.

2.3 Principle 2 – estimation and use of the Green's function

The second basic principle of TRA has to do with measuring the Green's function, *g(t)*, of a medium and using it to back propagate a recorded signal, $r_j(t)$, at a receiver location x_j, to the a location, x_s.

First let's consider the simplest case. Suppose we place a delta function, $\delta(t)$, source at that source location x_s and record the resulting motion of the medium at a receiver, $r_j(t)$, in the medium. Because we have used a delta function source, the recorded motion is a direct measurement of the Green's function of the medium, $g_j(t)$, between the source location and the receiver location.

$$r_j(t) = \delta(t) * g_j(t) = g_j(t)\,. \qquad (1)$$

On the other side, the source-receiver reciprocity tells us that the source and receiver may (under some conditions) be interchanged with no change in the transfer function, i.e. if we place a delta function at the receiver location we can record the same $g_j(t)$ at the source location.

Unfortunately, we can never actually inject a delta source function in either numerical or physical experiments to measure the Green's function. We need to use a band limited, casual source function, *s(t)*. So instead of measuring the Green's function, $g_j(t)$, we obtain as our recorded signal, $r_j(t)$,

$$r_j(t) = s(t) * g_j(t)\,. \qquad (2)$$

Now if we are trying to back propagate the wave field like we do when we reverse the movie, we first reverse our recorded waveform, $r_j(t)$, and then propagate it from the receiver towards the source. Because the transfer function from the receiver to the source is the same $g_j(t)$ according to reciprocity, the desired signal, $\hat{s}_j(t)$, recorded at the original source location, x_s, is given by

$$\hat{s}_j(t) = r_j(-t) * g_j(t) = s(-t) * g_j(-t) * g_j(t)\,. \qquad (3)$$

This signal, $\hat{s}_j(t)$, can be seen as one back-propagation of the recorded signal, $r_j(t)$, at the source location through the TRA operation. Given we have infinite number of receivers on an enclosed contour surrounding the source, by performing the same process for all recorded signals and summing them up, we can obtain the signal that would have been recorded at the source location:

$$\hat{s}(t) = \sum_j \hat{s}_j(t) = \sum_j s(-t) * g_j(-t) * g_j(t) = s(-t) * \sum_j g_j(-t) * g_j(t) = s(-t)\,. \qquad (4)$$

It is clear that the correct estimation of the Green's function $g_j(t)$ is crucial to this back-propagation process. However, usually an exact calculation of this Green's function involves lots of complexity. Therefore, instead of using the exact Green's function, we use the recorded signal itself as an "empirical Green's function". In that sense, we must convolve the recorded signal, $r_j(t)$ with its time reversed version, $r_j(-t)$, giving

$$\begin{aligned}\tilde{s}_j(t) &= r_j(-t) * r_j(t) \\ &= [s(-t) * g_j(-t)] * [s(t) * g_j(t)] \\ &= [s(t) * s(-t)] * [g_j(t) * g_j(-t)]\end{aligned} \qquad (5)$$

We see that we have accomplished the back propagation of the energy from this receiver to the source location with only one complication (compare equation (3) and (5)) – we end up with the autocorrelation of the original source function, *s(t)*. We also know that the convolution of a trace with the time reverse of itself is identical to the autocorrelation of the trace. Thus it is easy to back propagate any trace from its recorded location to the original source location by only performing its autocorrelation. However, we will have to correct the source wavelet shape by a deconvolution process.

Equation (5) shows how to back propagate a single recorded trace from its receiver location back to the source location using the empirical Green's function. We must now perform this same task for all recorded traces on the contour which encloses the source. This is a simple matter of summing the autocorrelations for all individual receivers of a common source. If *N* is the number of receivers, the back propagated signal at the source location is given by

$$\tilde{s}(t) = \sum_{j=1}^{N} r_j(-t) * r_j(t) = s(t) * s(-t) \qquad . \qquad (6)$$

The limitation in practice of this methodology is how much of the enclosed contour around the source is actually captured by the seismic field acquisition. For surface seismic acquisition this may be a seriously limiting factor – we may not have captured the required energy by the surface receivers in order to apply this method. However, as we will show below, for walk away VSP acquisition it may be quite adequate.

2.3 Principle 3 – interpretation of the back propagated signal

In all of the literature we have surveyed, the value of the back propagated signal is limited only to times near the origin, that is when the source fired. Claims seem to be made that at all other times the energy cancels out. While indeed the energy at zero time is large, this trace contains the recorded reflections that would have been observed at the source location from all scatterers or reflectors in the medium. In other words, the back propagated signal at the source location is as if we had a receiver collocated at the source giving us a zero offset trace. This trace is the equivalent of the stacked trace at this source location. The great value of this point is that simply summing the autocorrelations of appropriate sets of traces, we obtain the zero offset stacked trace without any of the complexity of velocity analysis, normal moveout corrections, and muting.

3. VSP Velocity Model and Synthetic Seismic Traces

To demonstrate the use of TRA for imaging a salt dome flank, we built a 2-D salt dome velocity model, shown in Figure 2, using simplified velocities from the SEG/EAGE 3-D salt model (Aminzadeh et al., 1997). The overall model dimensions are 10km in width (x direction) by 5km in depth (z direction). The velocity model is sampled at a 5 meter grid spacing and the source used is a 30 Hz center frequency Ricker wavelet. The background velocity is described by a compaction gradient of the form given by

$$V(z) = V_0 + z \cdot K \ , \qquad (7)$$

where V_0 is the initial velocity of the top layer and K is the velocity gradient. The salt dome is a mushroom-shaped diapir that sits on the right side of the model with salt velocity taken as 4481m/s. Because we use a constant density and a smooth velocity gradient, there would be no sediment reflections observed. To remedy this, we introduce reflectors in the same manner as used in the SEG/EAGE salt model. We also used the “spike” method to create horizontal sediment reflections, as shown on the right side of Figure 2. Five horizontal velocity “spikes” are distributed evenly in depth and using an increase in velocity of 15% above the corresponding background velocity.

The preferred processing geometry is to acquire a reverse VSP, with sources at multiple depth levels in the borehole and receivers at the surface. On the other hand the preferred field acquisition geometry is to use surface sources and down-hole receivers since down hole sources are still rather problematic. However the data is actually recorded, we may invoke reciprocity to sort the traces into an equivalent reverse VSP geometry. In order to minimize the amount of computation time required to generate the walk away VSP data, we dodged the need for reciprocity and directly generated a reverse VSP using about 100 down-hole sources and about 400 surface receivers.

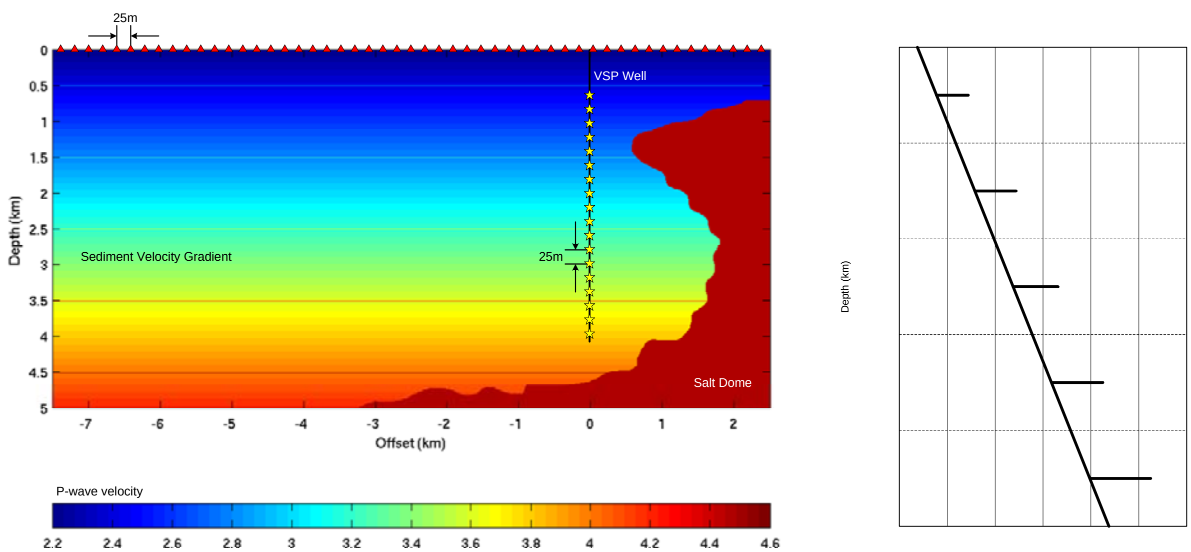

Figure 2. Salt dome velocity model - P-wave velocity profile (left), back ground velocity gradient (right).

The VSP well is located at x = 7.5km and the sources ranged from 1.6km to 4.1km with spacing of 25m. The 400 receivers are distributed along the surface with spacing of 25m. Figure 3 shows a common reverse VSP shot (or equivalently a common VSP receiver) gather. We used an elastic finite difference modeling algorithm and set the shear wave velocities to be very small. The left panel of Figure 3 shows the vertical component, v_z, of motion and the right panel shows the horizontal component, v_x.

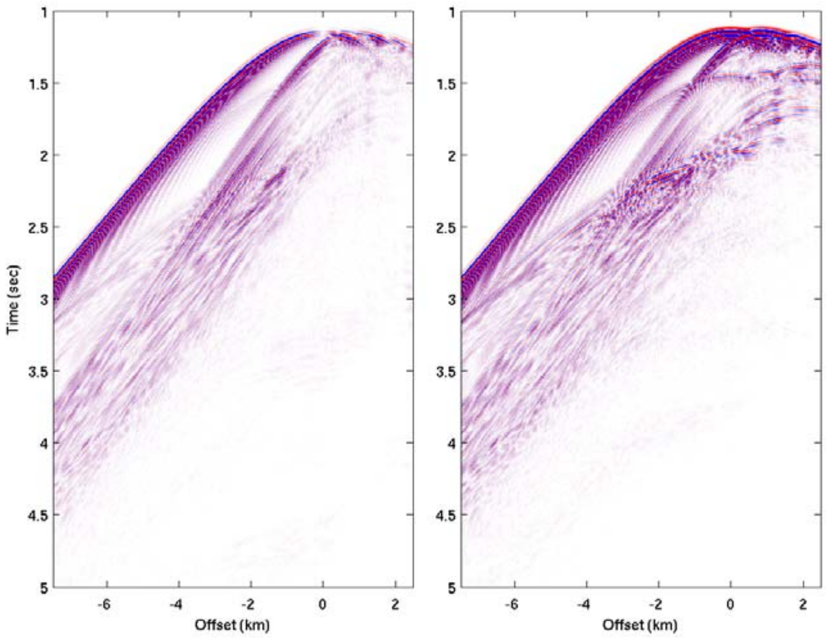

Figure 3. The horizontal component of motion, v_x, on the left panel and the vertical component of motion, v_z, on the right panel for one common shot reverse VSP (or equivalently one common depth level for a conventional VSP).

Due to the presence of the vertical velocity gradient, we will excite and capture turning ray energy. Specifically, reflections off the underside of the salt dome flank will be bent back toward the surface and be recorded on the surface receivers (or equivalently borehole sensors). Figure 4 shows a schematic of the turning ray information that we will capture. The use of turning ray energy is not new in and of itself and there have been many studies about using migration of surface seismic data to image the underside of salt domes using turning ray energy (e.g. Hale et al, 1992).

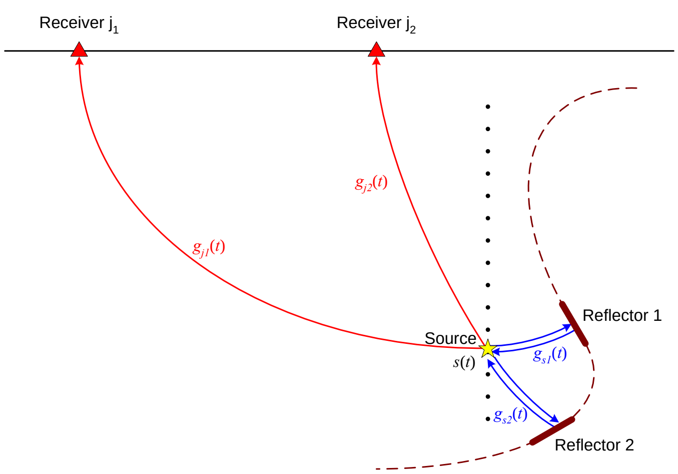

Figure 4. Schematic showing how the surface receivers will capture turning rays which have reflected off the underside of the salt dome flanks.

4. The Zero Offset Down-hole Acquisition Concept

Suppose it were possible to construct a down-hole VSP tool which had a coincident seismic source and receiver. If this tool were feasible to run, we could collect single fold, zero offset seismic data that would investigate the subsurface from the vantage point of the borehole.

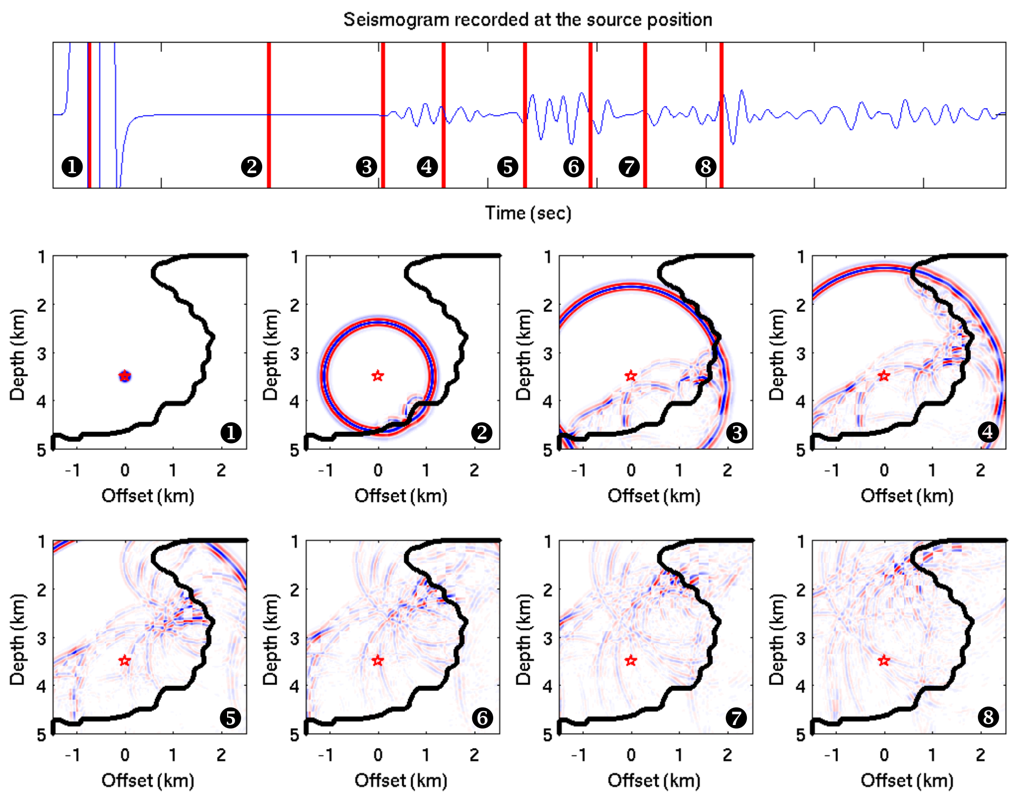

Figure 5. The bottom eight panels show successive snap shots of the wave field caused by a point source, indicated by the red star, firing at a depth of 3.5 km. The black line shows the outline of the salt dome. The top panel shows the wave form recorded at the source location. The time of each of the eight panels is indicated on the trace by the numerically labeled red bar.

Figure 5 shows the modeling results of just such a tool. The top trace shows the recorded wave field at the source location. Notice that at zero time, the amplitude is very large and off the scale of the plot. At later times we see many events. The lower eight panels show snap shots of the expanding wave field as a function of time. The time corresponding to each of the snap shots is denoted by the numerically labeled red vertical bar in the top panel. The panel labeled 1 is at a time just after the source fired. In panel 2 we see the wave field hit the bottom portion of the salt dome. In panel 3 we see that the reflections from the bottom of the salt dome are hitting the source position. We can see these reflections start just after the red vertical line labeled 3 in the top panel. In a similar manner, as each reflection off the salt comes back to the source location, we see the waveform on the top trace.

The point of this illustration is to show that the trace recorded at the source position will contain important information about the reflections off the salt dome flanks. Granted it will record the source wavelet at zero time, but it also contains reflected energy at later times which can be used to create an image of the salt. In the next section we will describe the results of back propagating the VSP data to each source location and then using these traces to image the salt dome flank.

5. Processing Methodology

The basic tasks we need to perform are to first back propagate the recorded VSP data to each sensor position in the borehole, and then migrate the traces to their proper position in the subsurface. A more detailed series of steps are as follows:

1) Organize the VSP data into the proper gathers. If the data were recorded as a conventional walk away VSP, then resort the data into the equivalent of a reverse VSP dataset. To do this, sort the traces into common VSP geophone gathers and call these "common reverse VSP shot gathers". If the data were collected as reverse VSP data, then the data are naturally in common reverse VSP shot gathers.

2) For each common shot gather, sum the auto-correlations of each trace. This operation produces the down-hole, zero offset stacked trace along the well bore at each VSP instrument depth.

3) Perform conventional post stack reverse time depth migration on the zero offset stacked traces to produce an image of the salt dome flank. This is the first time we use a velocity field – just the back ground vertical gradient without any salt and "spikes" in the model.

6. Results

The top two panels in Figure 5 show the back propagated zero offset VSP traces. For reference, each one of the traces in these panels came from the sum of the autocorrelations of the traces in a common shot record like Figure 3. The left panel shows the results for the horizontal component and the right panel shows the results for the vertical component. To check the accuracy of this methodology, the bottom two panels in Figure 5 show the corresponding actual zero offset traces created during the modeling. We see that they are remarkable the same with the back propagated traces showing noise, especially at early times. Some of this noise is in the form of coherent lineations which needs to be investigated further. Overall, however, we are encouraged that the methodology is working.

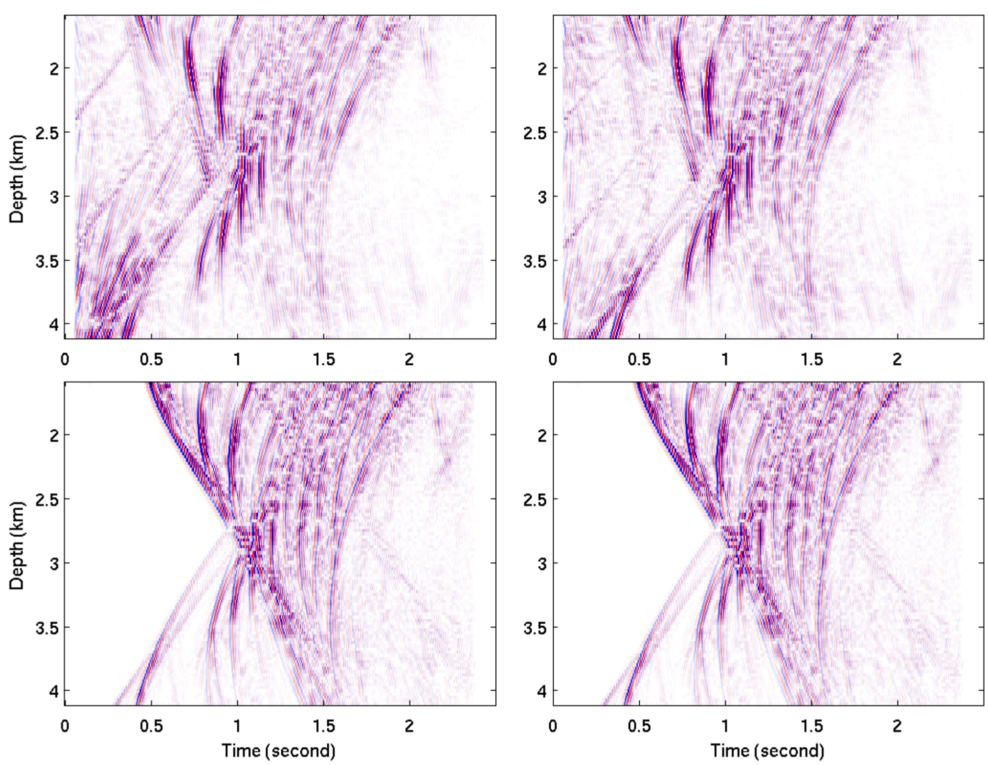

Figure 5. Comparison between the back propagated VSP traces (top) and the actual signals recorded by the receivers located at the source positions (bottom). The left column shows the horizontal component, Vx, and the right column shows the vertical component, Vz.

The middle panel in Figure 6 shows the result of performing a conventional post stack reverse time depth migration on the back propagated traces in Figure 5. We have combined the two vertical and horizontal components into an equivalent pressure response. The left panel shows the result of depth migrating the actual zero offset traces, while the right panel shows the correct velocity model. Our back propagated image has done a very good job of recreating the outline of the salt flank. It has not done a good job of recreating the horizontal layers and for some reason has created migration smiles out of them. It could be that this energy was not fully captured by the surface receiver array.

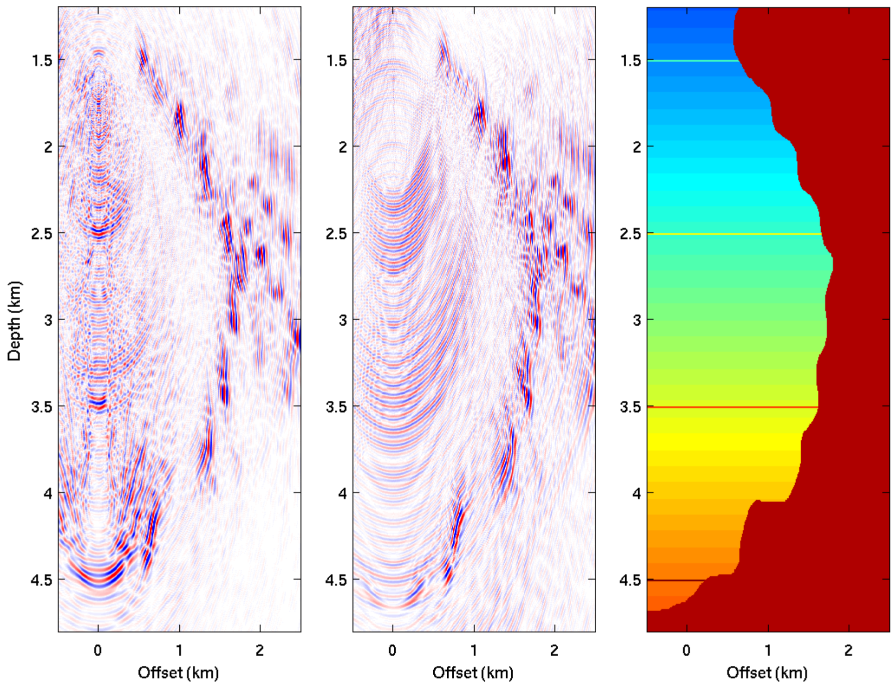

Figure 6. Comparison between the final migrated images from the back propagated VSP traces (middle) and the actual signals recorded by the receivers located at the source positions (left). The right panel shows actual velocity model. It is clear to see that the result from the back propagated data (middle) has imaged the salt flank almost as clearly and accurately as the actual zero offset data (left).

7. Summary

We extended the time reverse acoustics (TRA) methodology to an exploration seismic application of a multi-level, walk away VSP. The TRA concepts allow us to back propagate the recorded VSP data to a zero offset, down-hole reflection seismic experiment. Contrary to most of the TRA literature, we assert that the zero offset trace contains important imaging information that is normally discarded or ignored by these studies. The back propagation is accomplished with simple autocorrelations and without the use of any velocity analysis, normal move out corrections, or muting. This makes it possible to perform this type of processing during field acquisition in a fully automated fashion. The results we have obtained on acoustic model data suggests that the method may be very effective for processing VSPs collected in the Gulf of Mexico where turning rays provide reflections from the undersides and flanks of salt domes.

Images created by performing conventional, reverse time depth migration of the back propagated, zero offset data show clear definition of the salt dome flanks. These images are in good agreement with those created from actual zero offset traces and provide strong encouragement about the value of this methodology for locating the lateral extent and dimensions of salt dome flanks, especially in the Gulf of Mexico.

8. Acknowledgements

This work was supported by the Earth Resources Laboratory Founding Member Consortium.

References

Aminzadeh, F., Brac J., and Kunz T., 1997, SEG/EAGE 3-D Salt and Overthrust Models.

Baysal, E., Kosloff, D.D. and Sherwood, J, 1983, Reverse time migration, Geophysics 48, 1514-1524.

Borcea, L., and Papanicolaou, G., 2002, Imaging and time reversal in random media, Inverse Problem, 18, 1247-1279

Chang, W., and McMechan, G. 1987, Elastic reverse-time migration, Geophysics, 52, 1365-1375

Derode, A., Tourin, A., and Fink, M., 2000,, Limits of time-reversal focusing through multiple scattering: long range correlation, J. Acoust. Soc. Am. 107(6), 2987- 2998.

Draeger, C., Cassereau, D., and Fink, M., 1997, Theory of the time-reversal process in solids, J. Acoust. Soc. Am. 103 (3), 1289-1295.

Fink, M., and Cassereau, D. 2000, Time reversed acoustics, Rep. Prog. Phys., 63, 1933-1994

Fink, M. and de Rosny, J., 2002, Time-reversed acoustics in random media and chaotic cavities, Nonlinearity 15, R1-R18.

Hellman, K., Willis, M. E. and Young, T. K., 1986, Evaluation of a Reverse-Time Prestack Migration Algorithm, Presented at the 56th Ann. Internat. Mtg., Sot. Explor. Geophys.

Hale, D., Hill, N.R., and Stefani J., 1992, Imaging salt with turning seismic waves, Geophysics, **57**, 1453-1462.

Jonsson, L., Gustoafsson, M, Weston, V. and de Hoop, M., 2004, Retrofocusing of acoustic wave fields by iterated time reversal, SIAM J. Appl. Math. 64, 1954-1986.

Levin, S. A., 1984, Principle of reverse-time migration, Geophysics, 49 (5), 581-583.

Lu, R. and Toksöz, M. N., 2004, Finite-difference simulations of time reversed acoustics in a layered earth model, MIT Earth Resource Lab Report.

O'Brien, M.J., and Gray, S.H., 1996, Can we image beneath salt?, The Leading Edge, **15**, 17-22.

Whitmore, N., 1983, Iterative depth migration by backward time propagation, Presented at the 53rd Ann. Internat. Mtg., Sot. Explor. Geophy